

Cyclopean Eye based Binocular Orientation in Virtual Reality

Zhenping Xia^{*,**} and Eli Peli^{**}

^{*}College of Electronic and Information Engineering, Suzhou University of Science and Technology, Suzhou, China

^{**}The Schepens Eye Research Institute, Massachusetts Eye and Ear, Department of Ophthalmology, Harvard Medical School, Boston, MA, USA

Abstract

Currently the individual variability in the Cyclopean Eye's position is not considered when presenting virtual reality content. We proposed a novel perceptual space model for virtual reality content based on the location of the Cyclopean Eye. The proposed methodology may improve the immersive viewing experience and interaction accuracy between virtual reality system and individual user.

Author Keywords

Cyclopean Eye; binocular orientation; virtual reality; vernier acuity.

1. Objective and Background

The awareness of self-position is central to the experience in virtual space. In stereo displays, our self-position awareness refers to the location of our Cyclopean Eye, an abstract eye representing the joint visual axis of both eyes by a single axis of perceived direction [1]. Although binocular vision is formed with the views from two eyes, the binocular information is fused to form a cyclopean view, which is a 2D scene presentation as if it was observed from a visual point that appears between the eyes [2].

The content for virtual reality (VR), whether real world environments captured using a 3D camera system or computer generated virtual scenes, implicitly makes the assumption that the Cyclopean Eye is located on the inter-ocular axis midway between the two eyes [1]. The violation of this assumption of Cyclopean Eye's location in an individual observer results in different perception from that designed by the VR content. Barbeito and Ono [3] compared four methods for locating the Cyclopean Eye introduced by Fry [4], Funaishi [5], Howard and Templeton [6], and Roelofs [7]. They found that Howard and Templeton's method has higher test-retest stability. Howard and Templeton's task had two stimuli at different distances from the subject. The far stimulus is fixed at a certain viewing angle, while the near stimulus was moved laterally in the subject's frontal parallel plane. The subject task is to adjust the near stimulus left or right until they appeared aligned with both eyes open [6].

To provide a VR experience and interaction which considers the individual variability in the position of Cyclopean Eye, we propose a novel, stereo display based, method for measuring the location of the Cyclopean Eye (section 2), and incorporating the location of individual Cyclopean Eye into the VR perceptual space model (section 3).

2. Measurement of Cyclopean Eye Location

Our methodology of locating the Cyclopean Eye is based on a modified (stereo display based) version of Howard and Templeton's (real world) task using a dual presentation with a yes/no response paradigm [8] in place of their adjustment method.

2.1. Measurement setup and procedure

The measurement setup is illustrated schematically in Figure 1. A stereo display system presents two narrow vertical bars at different depths. The standard narrow bar P_s (x coordinate position fixed) is presented at the screen plane (no disparity) at a horizontal viewing angle γ relative to Z axis and the perceived test bar P_t (x coordinate position variable) is presented in front of the screen with fixed pixel crossed disparity.

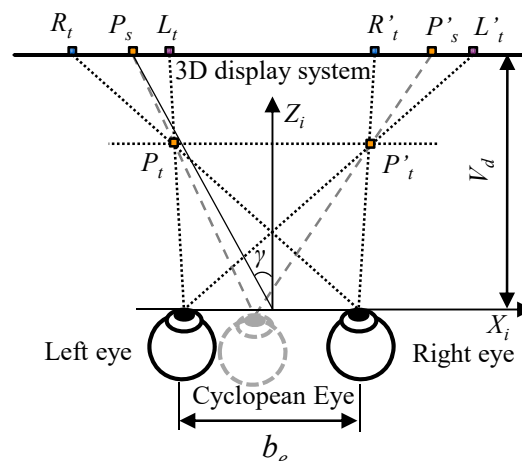


Figure 1. The stereo test for Cyclopean Eye locating, see Table 2 for symbols' meaning.

Using an adaptive psychophysical method [8], the next horizontal position of P_t to be tested is calculated based on subject's previous responses. The subject makes a judgment of whether or not the two narrow bars are aligned (yes/no paradigm). The axis joining P_s and the final P_t should include the Cyclopean Eye (up to a measurement error); using two axes from two different standard bars presented at two viewing angles can determine the location of Cyclopean Eye. Larger viewing angles differences should lead to smaller errors in Cyclopean Eye location. However, too large viewing angles will be uncomfortable due to the required larger angle of eye rotation and associated involuntary head rotation to the visual target. Hence, the viewing angles in the measurement were set to $\pm 15^\circ$. The display viewing distance was 65cm and the stereo depth of test narrow bar was limited to 0.67° cross disparity (7cm in front of the screen) to avoid discomfort that may be caused by the conflict between vergence and accommodation demands [9].

We used a Wheatstone mirror stereoscopic system, though the measurement can be implemented on any other stereo display system.

2.2. Methods

Four subjects participated in the pilot study. All subjects had normal or corrected to normal visual acuity (20/20 or better on Test Chart 2000 Pro, Thomson Software Solutions, London) and normal stereo acuity ($\leq 70''$) tested with random-dot stereograms on a clinical stereo vision testing chart (STERO OPTICAL CO., INC, Chicago, IL). Experiments were controlled by MATLAB script under Psychophysics Toolbox (Version 3).

The data was collected in a dual presentation: test bar above (standard bar below) and test bar below (standard bar above) intermixed. When the subject's response is that the test bar was subjectively misaligned with the standard bar, the test bar in the next trial is made closer by one step to the average positions of previous yes responses; if the bars judged to be aligned, the next test bar is moved two steps randomly to right or left with equal probability. By fitting psychometric functions with 288 judgments, from each presentation type, the point of subjective equality (PSE) is derived for the average location of P_t under specific viewing angle (γ) of P_s . The proportion of aligned (yes) response was counted for each placement of the stimulus and each presentation condition (Figure 2). For each presentation condition at a viewing angle, a psychometric function is fitted. The peak of psychometric function is the PSE under this condition. The average of the PSEs in both presentation conditions was taken as the final PSE. The

solid vertical lines in Figure 2 indicate the location of PSEs. The PSEs from the $+15^\circ$ and -15° were then transferred into horizontal (X direction) deviation of test bar (left and right views) in centimeters. With the subjective aligned locations of the two test bars (P_t and P'_t) and the corresponding locations of standard bars (P_s and P'_s), the x and z coordinates of the Cyclopean Eye are derived for each subject according to Figure 1. These values for 4 subjects are presented in Table 1. Also presented in Table 1, the average Cyclopean Eye position of 14 subjects collected by Barbeito and Ono [3] using Howard and Templeton's task are shown for comparison.

Table 1. The location of Cyclopean Eye.

Subject	$x_e (cm)$	$z_e (cm)$
#1	-0.068	-1.88
#2	0.075	-1.38
#3	0.69	-1.29
#4	0.64	-1.84
B&O[3]	0.28	-1.16

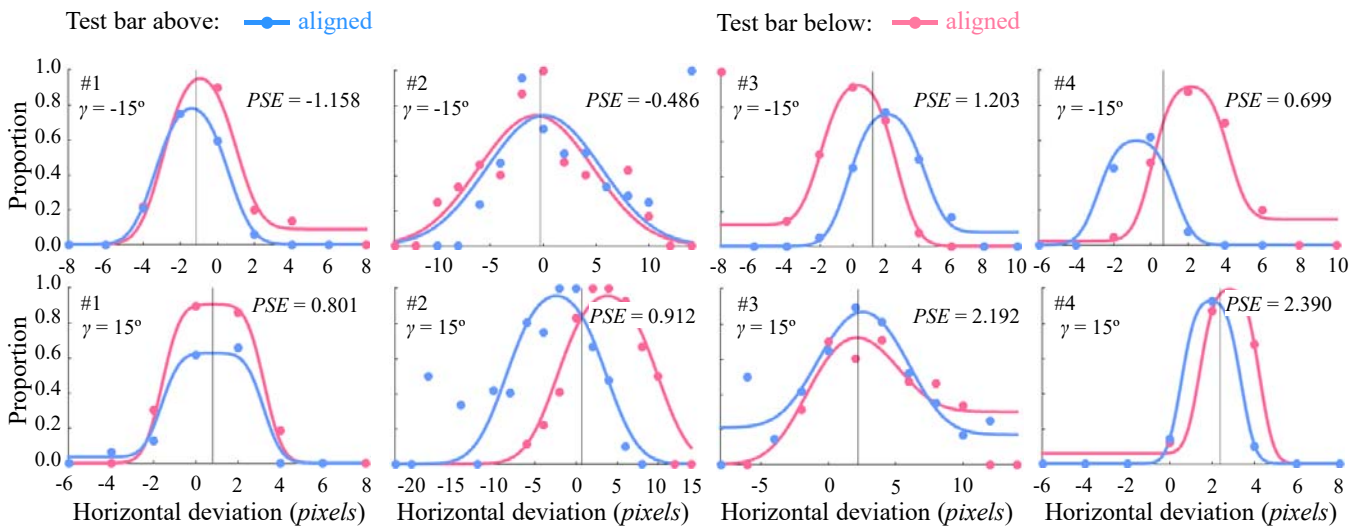


Figure 2. Psychometric functions under each presenting condition (test bar above or below standard bar) at two viewing angles $+15^\circ$ and -15° . The solid vertical line indicates the location of the PSE which is the average of two Psychometric function peaks obtained in the two presenting conditions.

3. Cyclopean Eye based perceptual space

The relationship between VR content acquisition and display parameters affects the final viewing experience. Since the parallel camera configuration (Figure 3a) and binocular parallax based stereoscopic display (Figure 3b) are commonly used systems [9-10], the geometry model of Cyclopean Eye-based perceptual space will be established based on them.

The geometry of Cyclopean Eye corrected VR content perception can be summarized as two main coordinate transformations. The first step is transformation from object space (X_o, Y_o, Z_o) to image space (X_i, Y_i, Z_i). A "Cyclopean Camera" is defined similarly to the "Cyclopean Eye", and is located at the midpoint between two

equal cameras (Figure 3a). The image space takes the inter-ocular axis midway between two eyes as the origin point of the coordinates (Figure 3b). Transformation between object space and image space goes through the camera sensor and display screen coordinates conversion with equations 1 to 3 [10]. With the parallel camera configuration, there is no difference in Y coordinates between the left and right views of the cameras or on the screen. With the equal configuration of field of view, convergence distance, and base line length between VR content acquisition and display systems, the object space and image space can be perfectly matched.

$$\begin{bmatrix} X_{cl} \\ X_{cr} \\ Y_c \end{bmatrix} = \begin{bmatrix} f \cdot (b_c + 2X_o) / (2Z_o) - s \\ -f \cdot (b_c - 2X_o) / (2Z_o) + s \\ f \cdot Y_o / Z_o \end{bmatrix} \quad (1)$$

$$\begin{bmatrix} X_{sl} \\ X_{sr} \\ Y_s \end{bmatrix} = \frac{W_s}{W_c} \cdot \begin{bmatrix} X_{cl} \\ X_{cr} \\ Y_c \end{bmatrix} \quad (2)$$

$$\begin{bmatrix} X_i \\ Y_i \\ Z_i \end{bmatrix} = \begin{bmatrix} b_e \cdot (X_{sl} + X_{sr}) / [2 \cdot (b_e - X_{sr} + X_{sl})] \\ Y_s \cdot b_e / (b_e - X_{sr} + X_{sl}) \\ V_d \cdot b_e / (b_e - X_{sr} + X_{sl}) \end{bmatrix} \quad (3)$$

$$\begin{bmatrix} X_p \\ Y_p \\ Z_p \end{bmatrix} = \begin{bmatrix} X_i \\ Y_i \\ Z_i \end{bmatrix} - \begin{bmatrix} x_e \\ y_e \\ z_e \end{bmatrix} \quad (4)$$

The second step is the transformation from image space to perceptual space (X_p, Y_p, Z_p) while considering the location of Cyclopean Eye (see equation 4).

4. Impact analysis

The orientation sensitivity in the 3D space may be expressed as vernier acuity measured positional offset between two objects at different distances from the observer. The vernier acuity exceeds the sampling limits of eye's optics and photo-receptors even in this 3D case [11].

The effect of Cyclopean Eye location shift is illustrated for one example in Figure 4a. Two ping pong ball sized spheres in the object space (real world) are shown in the perceptual space to show the effect of two different positions of the Cyclopean Eye. The blue spheres are simulated under the assumption that Cyclopean Eye is located at the midpoint of the eyes. The near and far blue spheres have no orientation difference and are perfectly aligned. The red spheres are simulated with the Cyclopean Eye's location shifted 1cm towards the right eye on the X-axis. The difference in orientation offset of the red spheres is obvious (Figure 4a) and is shown for different Cyclopean Eye position at the intersection of the curves with the vertical line at $Z=15cm$ in Figure 4b. Human vision is sensitive to the relative orientation offset and rigid object distance (from the near sphere to observer in the Z direction) changes the relative orientation offset of the two spheres (Figure 4b). In Figure 4b, the distance between two spheres is fixed as 15cm in Z direction. In this situation, two spheres are located in different depth planes and the vernier disparity between them varied with varying stereo-disparity. The vernier acuity threshold for such target is 34 arc sec [12] (reference line in Figure 4b). For conditions where the curves in Figure 4b are above the vernier threshold, the directional difference will be visible when the objects move in the Z directions, and appear as a distortion of the rigid object. Such distortion due to movement may be a source of visually induced motion sickness. The 34 arc sec was measured with static targets. If the threshold is

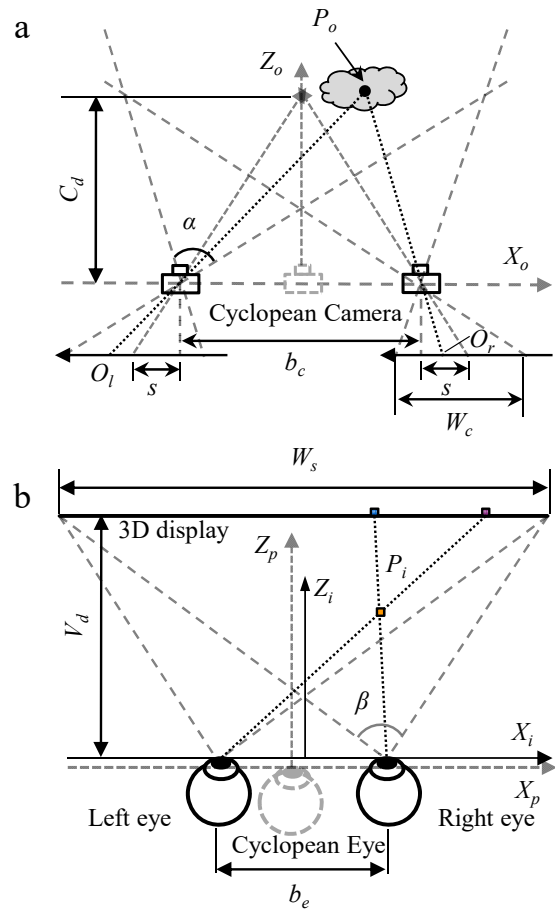


Figure 3. VR content acquisition, display and perception. (a) Natural world scene acquisition with parallel camera configuration; (b) virtual world presenting and perception. See Table 2 for symbols' meaning.

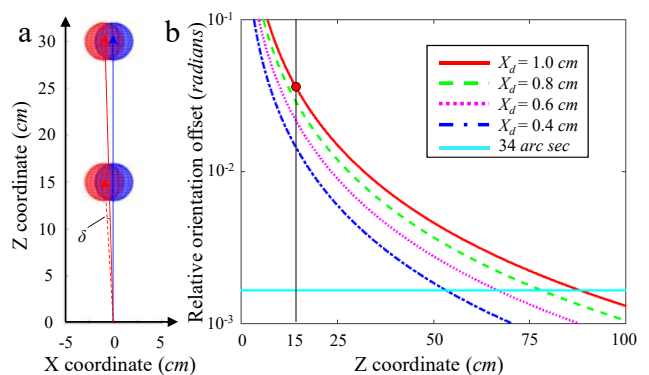


Figure 4. Effect of the Cyclopean Eye location. (a) Two spheres in the object space are shown to the perceptual space with different positions of Cyclopean Eye; (b) relative orientation offset of two spheres (15cm apart from each other in Z direction) in the perceptual space with different Cyclopean Eye locations X_d (deviation from the midpoint of the eyes in X direction) and distances (from the near sphere to observer in Z direction).

lower for moving objects the range will be increases, if the threshold is higher the range will shrink and may not be consequential. The Vernier detection threshold in motion is yet to be determined.

5. Conclusion

To improve the immersive viewing experience and interaction accuracy in virtual reality, the individual variability in the position of Cyclopean Eye can be considered. The individual location of Cyclopean Eye is measured using a stereo display. The possible effect on the user can be estimated and then the perceptual space model based on the location of Cyclopean Eye may potentially be adjusted to compensate for this individual effect.

6. Acknowledgement

This research is supported by the China Scholarship Council (CSC file No. 201704515003) and by a Faculty Research Awards from Google Inc. to Dr. Peli.

7. References

- [1] J. Turski, "On binocular vision: The geometric horopter and Cyclopean eye," *Vision Res.*, vol. 119, pp. 73–81, 2016.
- [2] L. Jin, A. Boev, K. Egiazarian, and A. Gotchev, "Quantifying the importance of cyclopean view and binocular rivalry-related features for objective quality assessment of mobile 3D video," *EURASIP J. Image Video Process.*, vol. 2014, no. 1, p. 6, 2014.
- [3] R. Barbeito and H. Ono, "Four methods of locating the egocenter: A comparison of their predictive validities and reliabilities," *Behav. Res. Methods Instrum.*, vol. 11, no. 1, pp. 31–36, 1979.
- [4] G. Fry, "Visual perception of space," *Optometry & Vision Science*, vol. 27, no. 11, pp. 531–553, 1950.
- [5] S. Funaishi, "Weiteres über das Zentrum der Schrichtungen," *Albrecht von Graefes Archiv für Ophthalmologie*, vol. 117, no. 2, pp. 296–303, 1926.
- [6] I. P. Howard and W. B. Templeton, "Human spatial orientation," Oxford, England: *John Wiley*, 1966.
- [7] C. Roelofs, "Considerations on the visual egocentre". *Acta Psychologica*, vol. 16, pp. 226–234, 1959.
- [8] M. A. García-Pérez and R. Alcalá-Quintana, "The indecision model of psychophysical performance in dual-presentation tasks: Parameter estimation and comparative analysis of response formats," *Front. Psychol.*, vol. 8, p. 1142, 2017.
- [9] Z. Xia, C. Cheng, and X. Li, "Visual comfort enhancement study based on visual attention detection for stereoscopic displays," *J. Soc. Inf. Disp.*, vol. 24, no. 10, pp. 633–640, 2016.
- [10] A. Woods, T. Docherty, and R. Koch, "Image Distortions in Stereoscopic Video Systems," *SPIE's Symp. Electron. Imaging Sci. Technol.*, vol. 1915, pp. 36–48, 1993.
- [11] C. Hou, Y. Kim, and P. Verghese, "Cortical sources of Vernier acuity in the human visual system: An EEG-source imaging study," *J. Vis.*, vol. 17, no. 6, p. 2, 2017.
- [12] S. P. Heinrich, M. Kromeier, M. Bach, and G. Kommerell, "Vernier acuity for stereodisparate objects and ocular prevalence," *Vision Res.*, vol. 45, no. 10, pp. 1321–1328, 2005.

Table 2. Symbols used in this article.

Variable	Geometric meaning
(X_o, Y_o, Z_o)	Object space coordinates
(X_i, Y_i, Z_i)	Image space coordinates
(X_p, Y_p, Z_p)	Perceptual space coordinates
(x_e, y_e, z_e)	Position of Cyclopean Eye in Image space
(X_c, Y_c)	CCD plane coordinates, X_{cl} for left camera and X_{cr} for right camera
(X_s, Y_s)	Display Screen plane coordinates, X_{sl} for left view and X_{sr} for right view
α	Single camera view field
β	Single eye view field
γ	Viewing angle
δ	Orientation offset of two spheres
b_c	Base line length between cameras
b_e	Base line length between eyes
W_c	The width of camera sensor (CCD)
W_s	The width of display screen
C_d	Convergence distance of 3D camera system
V_d	Viewing distance of 3D display system
f	Focal length of camera
s	Camera sensor (CCD) offset for convergence
P_s	Standard bar
P_t	Test bar
R_t	Right view of test bar
L_t	Left view of test bar
P_o	Point in object space
O_l	Position of P_o on left camera sensor (CCD)
O_r	Position of P_o on right camera sensor (CCD)
X_d	Location of Cyclopean Eye in X direction